DOI: 10.15825/1995-1191-2023-4-109-120

BIOLOGICAL PROPERTIES OF MACROPOROUS CRYOSTRUCTURATE BASED ON EXTRACELLULAR MATRIX COMPONENTS

A.M. Grigoriev[1], Yu.B. Basok[1], A.D. Belova[1], N.P. Shmerko[1], A.M. Subbot[5], V.K. Kulakova[3], V.I. Lozinsky[3, 4], V.I. Sevastianov[1, 2]

[1] Shumakov National Medical Research Center of Transplantology and Artificial Organs, Moscow, Russian Federation
[2] Institute for Biomedical Research, Moscow, Russian Federation
[3] Nesmeyanov Institute of Organoelement Compounds, Moscow, Russian Federation
[4] Kazan Federal University, Kazan, Russian Federation
[5] Research Institute of Eye Diseases, Moscow, Russian Federation

Objective: to study the biological properties of macroporous cryostructurate from multicomponent concentrated collagen-containing solution (MCCS) as a promising matrix for the formation of cell- and tissue-engineered constructs. **Materials and methods.** A macroporous spongy carrier was obtained by cryostructuring of collagen-containing extract, prepared by acetic acid hydrolysis of chicken connective tissue (BIOMIR Service, Russian Federation). N-(3-dimethylaminopropyl)-N'-ethylcarbodiimide (Sigma-Aldrich, USA) was used to make the cryostructurate water insoluble. The micromorphology of the sponge surface was studied using scanning electron microscopy. The cytotoxicity of the carrier was evaluated by reaction of the mouse NIH 3T3 fibroblast cell culture using automated microscope IncuCyte ZOOM (EssenBioscience, USA). Biocompatibility of the macroporous carrier was studied on cultures of human adipose tissue-derived mesenchymal stromal cells (AD-MSC), human hepatocellular carcinoma cell line *HepG2* and human umbilical vein endothelial cell line *EA.hy926*. The metabolic activity of cells was determined using PrestoBlue™ reagents (Invitrogen™, USA). Cell population development during long-term cultivation of the cell-engineered construct (CEC) was assessed by fluorescence-lifetime imaging microscopy over the entire surface of the sample using a Leica Dmi8 inverted microscope with Leica Thunder software (Leica Microsystems, Germany). **Results.** Optical microscopy and scanning electron microscopy (SEM) showed the presence of pores of different sizes in the resulting biopolymer material: large pores with 237 ± 32 μm diameter, medium-sized pores with 169 ± 23 μm diameter, and small-sized pores with 70 ± 20 μm diameter; large and medium-sized pores were predominant. The studied media did not exhibit cytotoxicity. Cell adhesion and proliferation on the surface of the material and their penetration into the underlying layers during long-term cultivation were observed. The highest metabolic activity of the cells was observed for human AD-MSC on day 14, which corresponds to the normal dynamics of development of a population of cells of this type. The functional activity of HepG2 cells – albumin and urea production – was shown in the liver CEC model. **Conclusion.** The good adhesion and active proliferation that were shown for the three cell types indicate that the resulting biopolymer carrier is biocompatible, and that the spread of the cells into the inner volume of the sponge and active population of the sponge under prolonged culturing indicates that this material can be used to create cell- and tissue-engineered constructs.

Keywords: cryogenic structuring, collagen, tissue engineering.

INTRODUCTION

One of the most important aspects of creating cell-engineered constructs (CEC) and tissue-engineered constructs (TEC) is the selection of a suitable scaffold which, on one hand, performs a structure-forming function, and, on the other hand, influences cell proliferation and differentiation processes. The internal architecture of TEC and CEC has been shown to be of fundamental importance for their structural and biological functions [1]. For instance, the use of a carrier with an ordered structure of microfibers that set the direction of growth of mesenchymal stromal cells (MSCs) in cartilage TECs led to increased glycosaminoglycan synthesis during cell differentiation compared to an unstructured scaffold [2]. Its structure is of even greater importance for the creation of TECs and CECs of the liver, where the normal functioning of cells of different types is possible only if there is a certain microarchitecture of the structure [3, 4].

Corresponding author: Alexei Grigoriev. Address: 1, Shchukinskaya str., Moscow, 123182, Russian Federation. Phone: (499) 193-86-62. E-mail: Bear-38@yandex.ru

Various approaches such as electrospinning [5] and various types of bioprinting [6] are used to create structured cell carriers. Much focus is on the search for new bioprinting materials that mimic the extracellular matrix and methods of imparting a structure closer to the native tissue [7].

It should be noted that, despite the numerous advantages of these techniques, they are difficult to perform and require expensive equipment. In turn, the cryostructuring methodology allows to create effective scaffolds with pores of different sizes at lower costs, providing both mass transfer of nutrients and gases and expansion of cells from the surface into the inner volume of the scaffold material [8].

Cryostructuring techniques are used to obtain such macroporous polymeric materials as various cryogels and cryostructurates [9]. The former are formed when 3D polymer mesh nodes are formed in the volume of unfrozen microphase of a macroscopically frozen system (this process is called cryotropic gelation). If there is no gelation proper, then after removal of the frozen solvent, for example, by sublimation or cryoextraction, polymeric objects called cryostructurates are obtained. A fundamental feature of both cryogels and cryostructurates is their macroporosity formed by polycrystals of the frozen solvent. Most macropores are interconnected, and their morphology and sizes depend on the conditions of all successive stages of cryogenic structuring. It is this special macroporosity, combined in many cases with good mechanical properties of various cryogels and cryostructurates, especially those based on biocompatible polymers, that makes them promising materials for biomedical applications [10–15].

An important advantage of this technology is that the physical properties of cryogenically structured materials, especially the pore size, can be influenced quite easily by adjusting the preparation parameters, including polymer content, crosslinking mechanism, temperature, freezing time, and freeze/thaw rate and cycles [8, 16].

When choosing materials for the manufacture of CEC and TEC matrices, besides synthetic resorbable polymers such as polylactides [17], biopolymer hydrogels are most commonly used. Many hydrogels based on one of the extracellular matrix (ECM) components have been developed to stimulate the regenerative potential of damaged tissues by minimally invasive injection [18]. In this case, among commonly used biopolymers, preference is given to such natural polymers as collagen, gelatin, chitosan, hyaluronic acid, alginates, and polyesters of bacterial origin [19].

Given the multifunctional properties of ECM, the attention of researchers in recent years has been drawn to multicomponent biopolymer-based hydrogels – ECM biomimetics, which include all of its main components (proteins and polysaccharides) as well as growth factors and other signaling molecules necessary for cell adhesion, proliferation and differentiation [19, 20]. Such biopolymer-based hydrogels have been shown to provide greater cell proliferation compared to single ECM component substrates [21]. However, along with the pronounced advantages of hydrogels, there are several difficulties associated with the inability to perform the function of a scaffold for cells and the lack of sufficient pore space, which does not allow angiogenesis to proceed throughout the entire volume of CECs, complicates cell migration into the hydrogel volume, transport of nutrients to them, and removal of metabolites [10].

Consequently, the idea of creating a bioactive macroporous cryostructured matrix [22] that is based on a multicomponent concentrated collagen-containing solution (MCCS) obtained by acetic acid extraction from animal tissues seems promising [20].

This study is a continuation of our earlier works on obtaining and studying the physicochemical and biological properties of gelatine-based macroporous cryostructurate [23, 24]. The positive results obtained in the creation of CECs based on gelatin cryostructurate matrices allowed us to use them in this work as comparison samples.

MATERIALS AND METHODS

Preparation of MCCS-based cryostructured matrix

A commercially available product, "Collagen-containing extract" (TU 9389-008-54969743-2016, BIOMIR Service, Krasnoznamensk) was used as the initial raw material. MCCS level was 40 mg/mL, total protein content in the MCCS was 96%, pH = 5.8 ± 0.3. MCCS-based cryostructure samples were produced at the Nesmeyanov Institute of Organoelement Compounds in Moscow according to the modified method [22]. The MCCS was first heated for 1 hour at 42 °C, then diluted 1.5 times with deionized water and poured into 35 mm diameter plastic Petri dishes in a thin layer (2 mm). The dishes were placed in an ultracryostat K2 (Huber, Germany) and frozen at –20 °C for 3 hours. Then they were freeze-dried in a FreeZone[1] unit (Labconco, USA). Next, the resulting macroporous cryostructurate sponges were incubated in 0.1 M ethanol solution of N-(3-dimethylaminopropyl)-N'-ethylcarbodiimide (Sigma-Aldrich, USA) at room temperature for 24 hours. Afterwards, they were washed with ethanol to remove excess carbodiimide and stored in 96% ethanol medium until used as a matrix for cell culture. For experiments, disks of 1 cm^2 area and 2 mm thickness were cut from the macroporous sponges.

Investigation of surface micromorphology of cryostructurates

The surface morphology of the samples was studied by phase-contrast microscopy using a Leica DMi8 Thunder super-resolution system with LAS X software.

The micromorphology of the collagen-containing matrix surface was studied using scanning electron microscopy (SEM) with lanthanide contrast of the sample, which allowed using low vacuum conditions, preserving the native structure of the material as much as possible [25]. Sample preparation included initial washing, exposure for 45 minutes in BioREE-A contrasting solution (Glaucon LLC, Russia) and final washing with distilled water. Next, excess moisture was removed from the surface of the specimen with an air brush and placed on the slide of an EVO LS10 microscope (Zeiss, Germany). Observations were performed in low vacuum mode (EP, 70 Pa), at an accelerating voltage of 20–25 kV. Images were captured using a backscattered electron detector (BSE mode).

Cell cultures

To evaluate cytotoxicity of the tested matrices, we used mouse NIH 3T3 fibroblast cell line (ATCC®CRL-1658™) from the American Type Culture Collection (ATCC). To study cell adhesion and proliferation, we used of human adipose tissue-derived mesenchymal stromal cell (AD-MSC) culture obtained at Shumakov National Medical Research Center of Transplantology and Artificial Organs according to the previously developed method [23]. Human umbilical vein endothelial cell line EA.hy926 (ATCC®CRL-2922™) from ATCC and human hepatocellular carcinoma cell line HepG2 from the cell culture collection owned by Shumakov National Medical Research Center of Transplantology and Artificial Organs were used to create CEC sponges.

Cell cultures were stored in liquid nitrogen at –196 °C. After thawing, the cells were seeded into standard 25 cm^2 culture vials (CELLSTAR® Greiner Bio-One, Germany) and cultured in appropriate complete growth medium (CGM). For fibroblast cell lines NIH 3T3 and endothelial cell lines EA.hy926, high glucose DMEM (PanEco, Russia) supplemented with 10% fetal calf serum (TS, Biosera, Germany) or fetal calf serum (HyClone, USA), respectively, antibiotic-antimycotic Anti-Anti (Gibco® by Life Technologies™, SC) and 2 mmol alanyl-glutamine (PanEco, Russia) were used. AD-MSC and HepG2 were cultured in DMEM/F12 medium (PanEco, Russia) supplemented with 10% fetal calf serum (HyClone, USA), 10 μg/mL of basic human fibroblast growth factor (FGF-2, Peprotech, AF-100-18B, USA), antibiotic-antimycotic Anti-Anti (Gibco® by Life Technologies™, SC), 1 mmol HEPES (Gibco® by Life Technologies™, SC) and 2 mmols alanyl-glutamine (PanEco, Russia). Vials with cells were cultured in a CO_2 incubator under standard conditions: 37 °C, humid atmosphere containing (5 ± 1) % CO_2.

For experiments, cells were washed off the culture plate using dissociation reagent TrypLE™ Express Enzyme (Gibco® by Life Technologies™, SC) and a suspension with the required cell concentration was prepared.

Cell count in the suspension was determined on an automated cell counter (TC20™ Automated Cell Counter, BIORAD, Singapore) with simultaneous viability test with trypan blue (BIORAD, # 145-0013, Singapore) according to the equipment manufacturer's methodology.

Matrix cytotoxicity assessment

The cytotoxicity of samples of MCCS-based media was determined by direct contact method according to GOST ISO 10993-5-2011 [26]. Mouse NIH 3T3 fibroblast cell lines were seeded into flat-bottomed 6-well culture plates (CELLSTAR® Greiner Bio-One, Germany) at a concentration of 5×10^5 cells per well and incubated for 24 hours at 37 °C under standard conditions until the formation of (80 ± 10)%. Next, the studied samples of cryostructurates were placed on the surface of the cell monolayer in the form of disks with a diameter of 6 mm and a thickness of 2 mm. The comparison samples were macroporous sponges in the form of gelatin-based cryostructurate disks of the same size as the samples of collagen-containing cryostructurates with proven absence of cytotoxic effect [23]. The disks were first thoroughly washed of ethanol residues with two portions of sterile distilled water and left for 24 hours in CGM at 37 °C. The CGM served as a negative control sample for cell culture, and 10 mg/mL single-element aqueous zinc standard (Sigma-Aldrich, USA) served as a positive control sample).

An additional test was performed for more detailed evaluation of growth dynamics and to identify a possible cytostatic effect. During the test, cell plates were incubated in the presence of samples using the IncuCyte ZOOM system (EssenBioscience, USA). The IncuCyte ZOOM system allowed the monolayer density to be assessed automatically every 2 hours throughout the experiment with simultaneous construction of growth curves. The experiment lasted for just over 50 hours.

Assessing the ability of the sponge carrier to support cell adhesion and proliferation

The ability of MCCS-based cryostructurate to support cell adhesion and proliferation was also compared with gelatin-based cryostructurate samples. To set up the experiment, cryostructurate samples were thoroughly washed from ethanol and placed in a CGM for 1 day until saturation. The required number of cells was grown in culture vials and a cell suspension with a working concentration of 1×10^5 cells/mL was prepared. Next, 1 ml of the cell suspension was applied to the sample surface drop by drop. The samples were placed in 50 ml centrifuge tubes and left in a CO_2 incubator for 1 hour for cell attachment, after which the CGM level in the tubes was brought to 5 ml and culturing was continued under standard conditions. On days 1, 3, 6, 9 and 14 of cultivation, three portions of the CGM were taken for metabolic activity test with PrestoBlue™ HS Cell

Viability Reagent (Invitrogen™ by Thermo Fisher Scientific, USA) according to the reagent manufacturer's protocol. Spectrophotometry was performed on a Spark 10M tablet reader (Tecan, Austria) with Spark Control™ Magellan V1.2.20 software at two wavelengths, 570 nm and 600 nm. Data from optical absorption measurements were used to calculate the coefficient of metabolic activity (K) according to the formula:

$$K = \frac{117,216 \cdot Abs_{570} - 80,586 \cdot Abs_{600}}{155,677 \cdot Abs_{600} - 14,652 \cdot Abs_{570}} \times 100\%,$$

where Abs_{570} is the optical absorption at 570 nm, and Abs_{600} is the optical absorption at 600 nm.

Cell count corresponding to coefficient K obtained was determined in an auxiliary experiment, where certain amounts of cells were seeded into the wells of a plate and their metabolic activity was measured after one day. A calibration graph was plotted based on the measurement results, which allowed to bring the value K to the number of AD-MSCs.

CECs based on collagen-containing cryostructurates and different cell types

To create CECs based on MCCS macroporous sponge, suspensions of appropriate cultures were prepared at a concentration of 1×10^5 cells/mL. Gelatin cryostructurate samples were also used as a control. Matrices from cryostructurates were immersed in the suspension and processed for 1 hour on a laboratory shaker in orbital stirring mode at 40 rpm for uniform distribution of cells on the surface and penetration into the inner volume of the sample. The resulting CECs were cultured under standard conditions for 7 and 10 days for HepG2, and 7 and 15 days for EA.hy926.

Cell surface adhesion, nature of cell distribution over the sample volume, viability, morphology and proliferative activity were assessed by in vivo microscopy with fluorescent dyes Live/Dead® Viability/Cytotoxicity Kit (Molecular Probes® by Life Technologies™, USA) using Leica DMi8 Thunder microscope with LAS X software for analyzing the 3-d structure of the sample.

Functional properties of HepG2 hepatocellular carcinoma cells when cultured on an MCCS-based macroporous matrix

HepG2 cells (5×10^5 kL), were plated on $10 \times 10 \times 2$ mm fragments of MCCS (n = 10) and gelatin (n = 10) samples. The resulting CECs were cultured in CGM under standard conditions for 10 days. On day 10, albumin content in the culture medium was determined by enzyme-linked immunosorbent assay using Human Albumin ELISA Kit (Invitrogen™ by Thermo Fisher Scientific, USA). Culture medium from cells that were cultured on plastic in the same quantity was used as a control.

Ammonia metabolism rate was determined after 90 minutes of incubation with 1 mmol ammonium chloride (Sigma-Aldrich, USA) diluted in culture medium on day 10 of the experiment. The amount of urea in the medium was estimated on a KonelabPrime 60i biochemical analyzer (ThermoFisher Scientific, Finland).

Reliability of differences was determined using Student's t-test (SPSS 26). Differences were considered statistically significant at $p < 0.05$.

RESULTS AND DISCUSSION

Investigation of surface micromorphology of macroporous matrices

A microscopy of the samples revealed a porous structure of the material with numerous pores of different sizes (Fig. 1, a). Conventionally, the pores can be categorized into three groups by size: large (237 ± 32 μm), medium (169 ± 23 μm) and small (70 ± 20 μm). Thus, the MCCS-based cryostructured material is dominated by large-sized pores. In comparison, only medium-sized (169 ± 23 μm) and small-sized (70 ± 20 μm) pores were mainly present in the gelatin cryostructured material (Fig. 1, b). SEM images of the surface of both

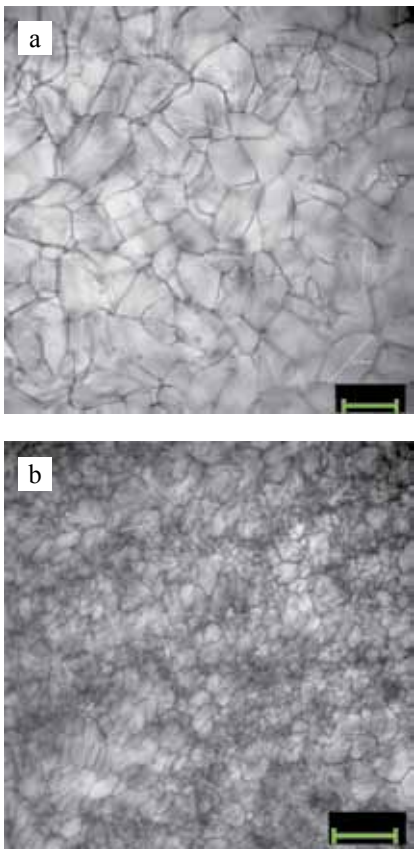

Fig. 1. Surface morphology of cryostructurates. Phase-contrast microscopy. Magnification 50×; a, MCCS-based cryostructurate; b, gelatin-based cryostructurate. Scale bar: 200 μm

sponges show that the pores form interconnected channels running through the entire volume of the material (Fig. 2).

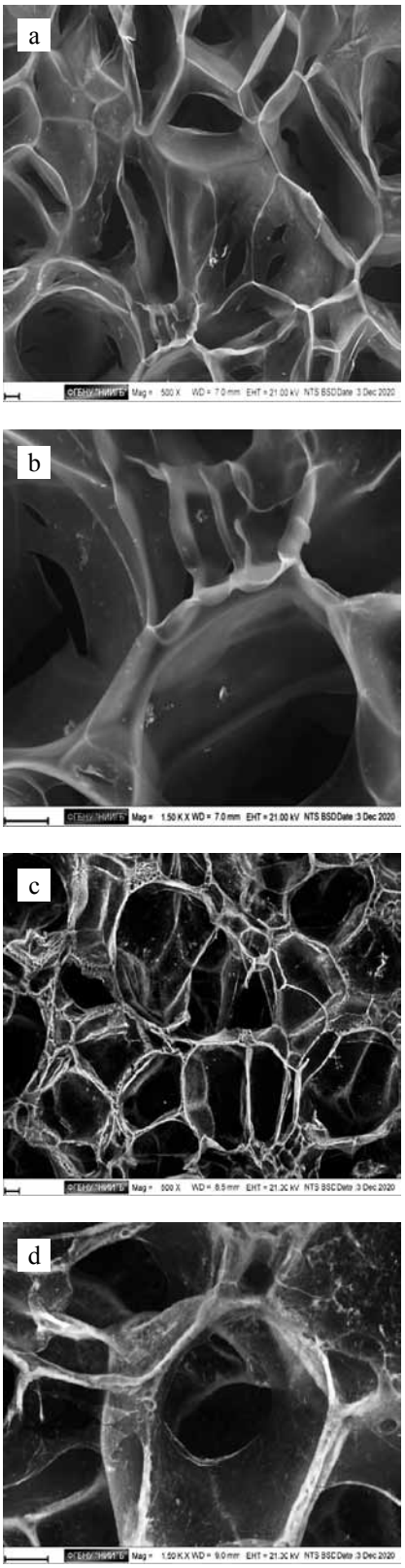

Fig. 2. Macroporous morphology of cryostructurates. SEM with lanthanide contrasting. a, b, MCCS-based cryostructurate; c, d, gelatin-based cryostructurate. a, b, magnification 500×; b, d, magnification 1500×. Scale bar: 20 μm

Cytotoxicity of the resulting cryostructurates

Assessment of the cytotoxicity of the MCCS-based cryostructurate revealed no negative effect when NIH 3T3 cells were cultured in the presence of fragments of macroporous matrices obtained from MCCS and gelatin. Cells actively proliferated over the entire area of the well of the plate, including the area of contact with the sample (Fig. 3). No rounded cells or cells with disturbed morphology were observed.

Determination of the degree of monolayer confluency in automatic mode showed that the most active cell growth begins after 20 hours of the experiment and, by the end of the experiment, this index reaches values of more than 70%, which corresponds to the normal development of NIH 3T3 cell population. There were no significant differences from the comparison sample (Fig. 3, b).

Biocompatibility. Cell adhesion and proliferation

The study of biocompatibility, i.e. the ability of cells to adhere to the surface and further proliferate, was carried out using an AD-MSC culture. In parallel, a gelatin-based cryostructurate was used as a control in the experiment. 1×10^5 cells were plated on a sponge fragment. Vital dye intravital microscopy showed that on day 3, cells adhered on the surface of both media. Distribution of AD-MSCs on the surface was quite uniform, the cells were spread out and had normal morphology. There were practically no dead cells. By day 12 of cultivation, a significant increase in cell mass was observed in the samples with the formation of large cell clusters. It was also noted that cells inhabited not only the surface of cryostructurates, but also penetrated deep into the sponge. Moreover, due to the presence of large, interconnected pores in the MCCS-based sponge, this effect was much more pronounced in this case (Fig. 4).

Data from the metabolic activity test with PrestoBlue™ reagent fully correspond to the microscopic picture and allow for quantitative assessment of their proliferative activity.

As shown in the graph (Fig. 5), after the lag phase that is necessary for cells to adapt, the logarithmic growth phase begins by day 4 of cultivation, and continues, with some slowdown by day 6–9, until the end of the experiment on day 14. In our opinion, the slowdown during this period is due to the filling of the available surface of the macroporous matrix by cells and the transition to colonization of the underlying layers of the cryostructurate. For both types of samples, we observed similar dynamics of cell mass growth, but AD-MSCs, when cultured on an MCCS matrix, proliferated more actively at late observation periods (days 9 and 14).

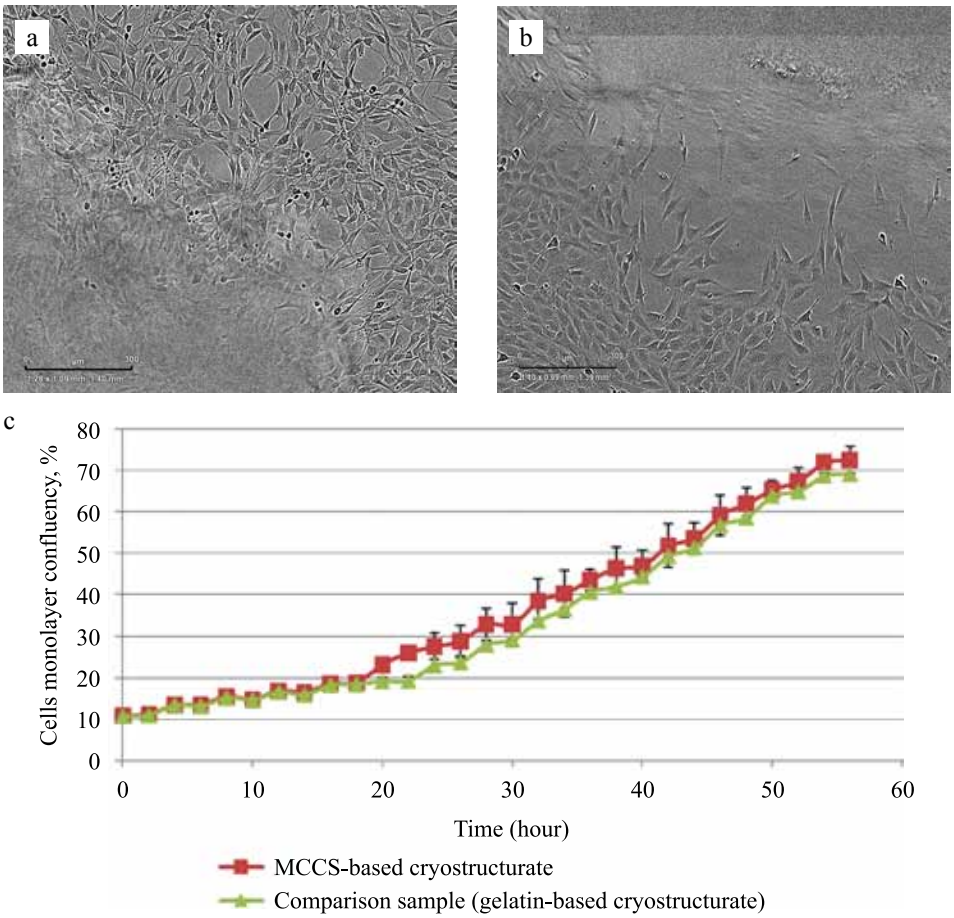

Fig. 3. Growth of mouse NIH 3T3 fibroblasts in the presence of macroporous matrix fragment. a, MCCS-based cryostructurate; b, gelatin-based cryostructurate (comparison sample). Phase-contrast microscopy. Magnification 100×. Scale bar: 300 μm; c, growth curve of NIH 3T3 cells on culture plastic in the presence of a fragment of MCCS-based macroporous carrier

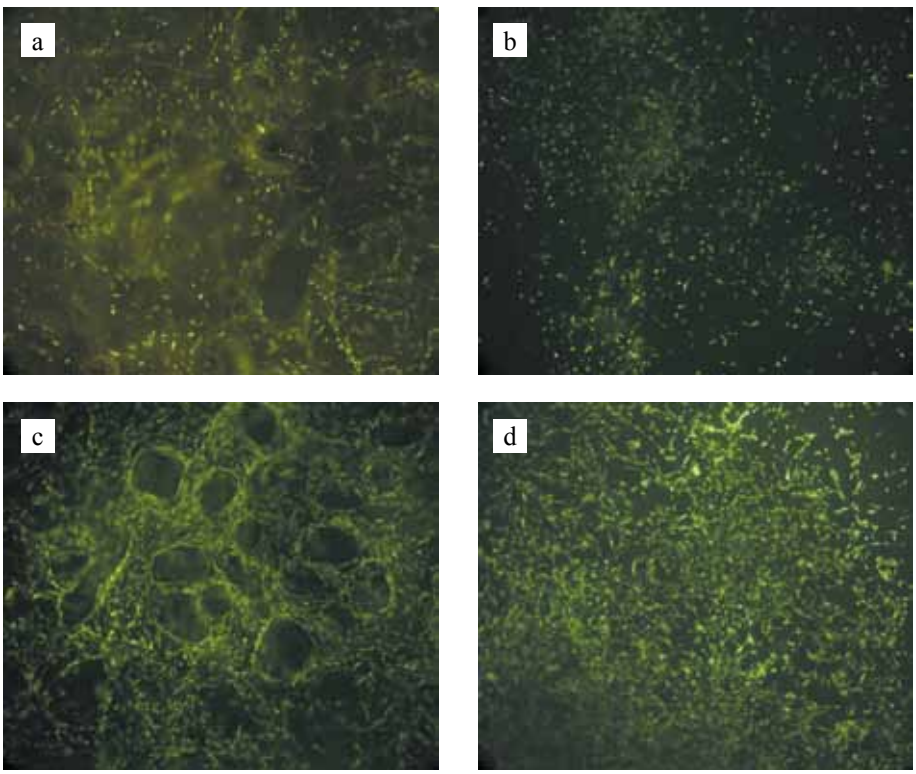

Fig. 4. Growth of human AD-MSC culture on MCCS-based matrix (a, c) and gelatin-based matrix (b, d); a and b, 3 days, c and d, 12 days of culture. Live/Dead™ stain. Magnification 100×. Scale bar: 100 μm

Creation of CECs from different cell types on an MCCS-based cryostructurate

When seeded with a large number of cells – 5×10^5 cells per sample – it was shown that for both HepG2 (Fig. 6, a–d) and EA.hy926 (Fig. 7, a–f) culture, almost all cells adhere to the sample surface and actively proliferate, forming significant clusters by the end of the experiment (on day 10 for HepG2, and day 15 for EA.hy926).

Adherent cells on gelatin-based cryostructurate also actively proliferated, but there were more dead cells in the case of HepG2 (Fig. 6, d). Note that significant differences were observed in the localization of cell clusters. In the case of the gelatin disk, we noted predominantly

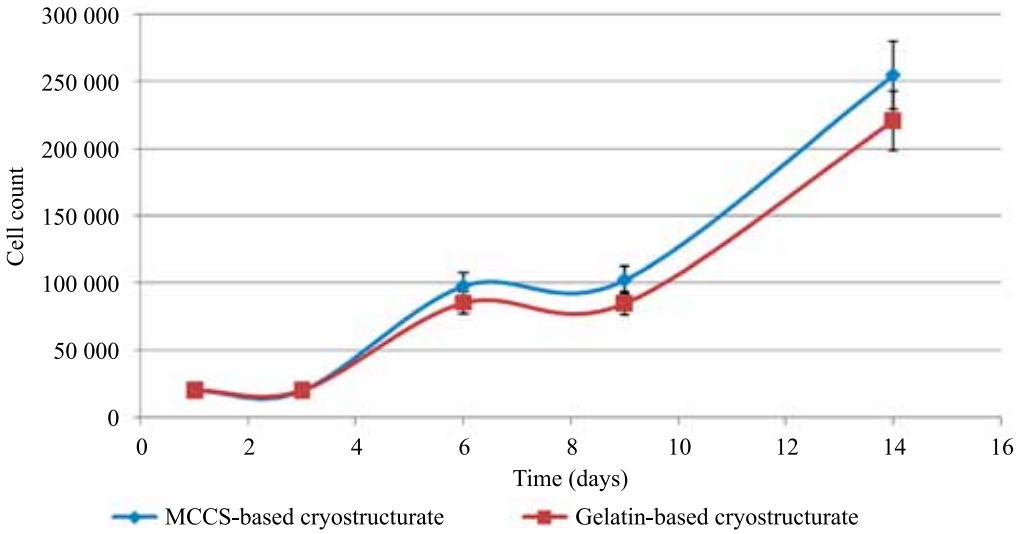

Fig. 5. Metabolic growth curve of human AD-MSCs on the tested matrices (Test with PrestoBlue™)

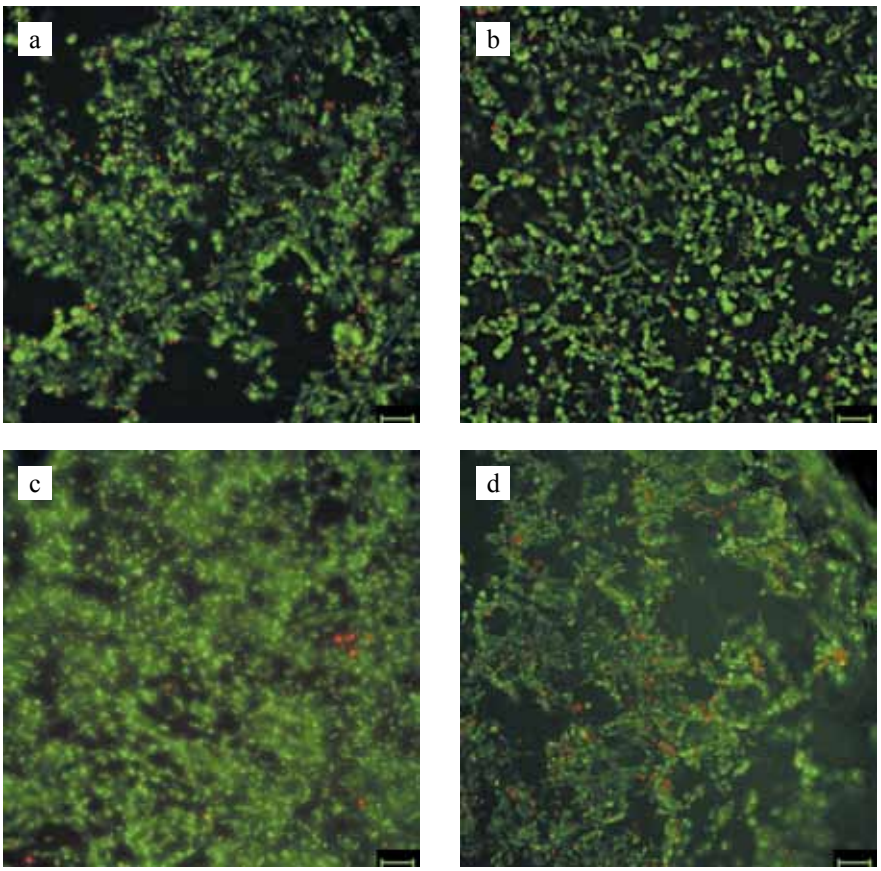

Fig. 6. HepG2 growth on a cryostructured matrix. a, 3 days of culture; b, 7 days, MCCS-based cryostructurate; c, 3 days of culture; d, 7 days, gelatin-based cryostructurate. Live/Dead™ stain, live cells are stained in green, dead cells are stained in red. Magnification 100×. Scale bar: 100 μm

cell spreading on the surface of the sample, whereas the MCCS disk showed a tendency to actively colonize the walls of large pores and channels with the colonization of the inner volume of the macroporous carrier. This was especially clear for endothelial cells at a late period of cultivation (Fig. 7, b).

The use of stacking technology", i.e. shifting the focal point of the microscope lens deep into the sample to a depth of more than 100 μm, followed by software processing of the image, showed that cells spread into the inner volume of the macroporous disk to a depth of up to 60 μm (Fig. 7, d).

For gelatin-based cryostructurates, this figure was smaller, not exceeding 50 μm (Fig. 7, e).

Assessment of the functional properties of HepG2 cells when cultured on an MCCS-based cryostructurate

The functional activity of HepG2 cells in CEC was analyzed by albumin synthesis and urea production

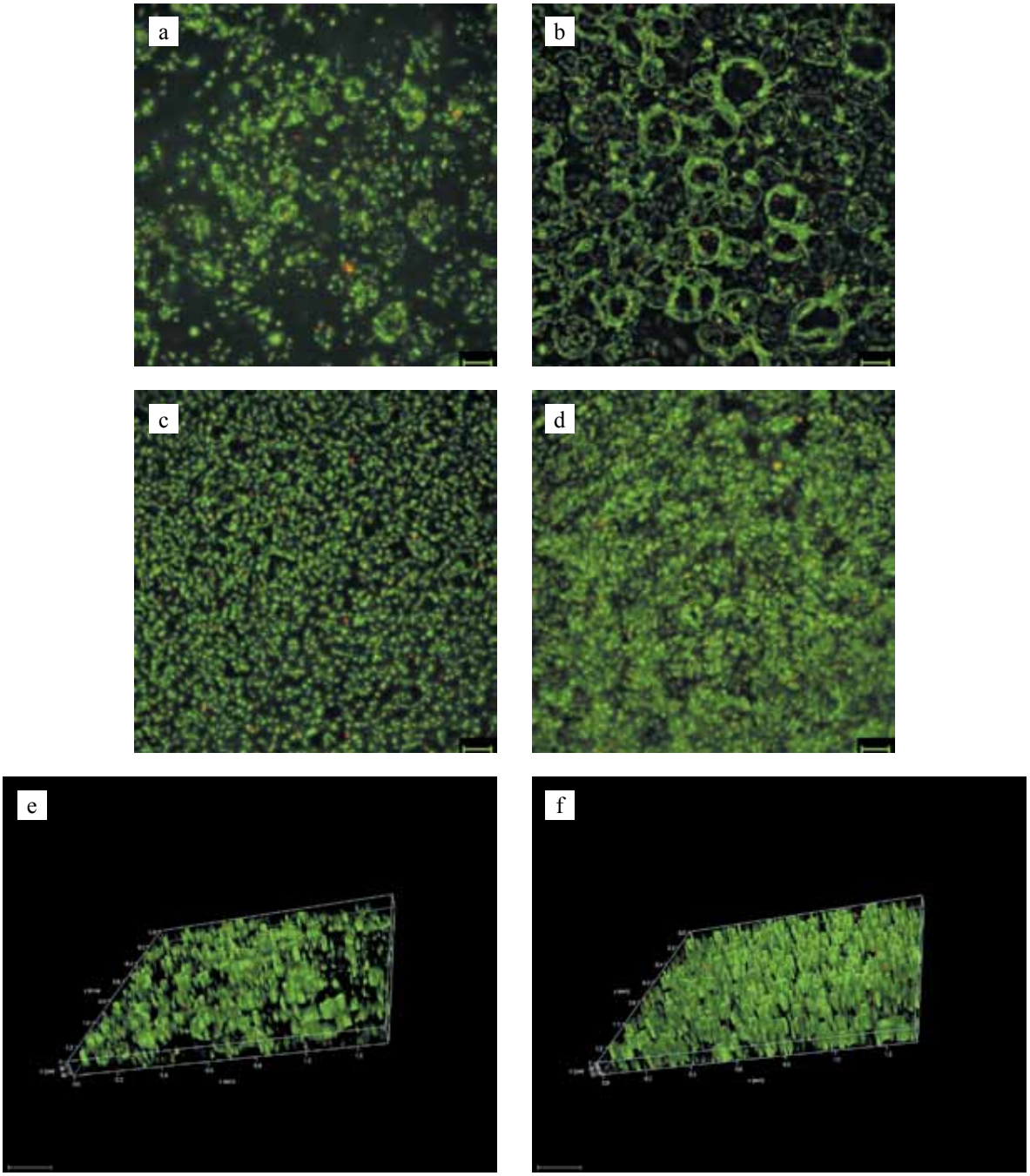

Fig. 7. EA.hy926 endothelial cell growth on cryostructured matrix. a, 7 days of culture; b, 15 days, MCCS-based cryostructurate; c, 7 days of culture; d, 15 days, gelatin-based cryostructurate; e, 15 days, cell distribution in the MCCS-based cryostructurate; f, 15 days, cell distribution in the gelatin-based cryostructurate. Live/Dead™ stain, live cells are stained in green, dead cells are stained in red. a–d, scale bar: 100 μm; e, f, scale bar: 200 μm

Table 1

Albumin content and urea level in culture medium on day 10 of culturing HepG2 cells on culture plastic (control)

	Albumin (mmol/mL)	Urea (mmol/mL)
Culture on plate (control)	960 ± 102	1.2 ± 0.2
Culture on MCCS-based cryostructurate	1413 ± 183	1.7 ± 0.3
p	<0.050*	0.051

* – the differences are statistically significant ($p < 0.05$).

Table 2

Albumin levels in culture medium on day 10 of CEC cultivation with different amounts of HepG2 cells

Cell count in CEC	Albumin (mmol/mL)
100,000	1323 ± 164
500,000	1413 ± 183
1,000,000	1963 ± 293

(Table 1). The culture medium of the same cell count on culture plastic was used as a control.

In a separate test, we compared the level of albumin production for CECs with different cell counts (Table 2).

Note that albumin and urea levels in the samples correlated with cell count in the CEC.

The obtained data indicate that HepG2 seeded on a MCCS-based cryostructurate can maintain its secretory function on day 10 of cultivation at a higher level, compared to cell cultivation on plastic.

CONCLUSION

The studies show that the macroporous cell carrier based on a cryostructured multicomponent concentrated collagen-containing solution has a large pore space, where large and medium-sized pores predominate, forming a network of branched channels in the matrix thickness. This macroporous structure significantly improves cell expansion deep into the MCCS-based cryostructurate compared to gelatin-based cryostructurates. The cell carrier studied in this work is non-cytotoxic, supports adhesion and proliferation of different cell types and formation of a cell-engineered construct in which cells can function normally.

The authors declare no conflict of interest.

REFERENCES

1. Transplantologija i iskusstvennye organy: uchebnik / Pod red. akad. RAN S.V. Gautier. M.: Laboratorija znanij, 2018; 319: il. (In Russ.).
2. *Yamamoto T, Randriantsilefisoa R, Sprecher CM, D'Este M*. Fabrication of collagen-hyaluronic acid cryogels by directional freezing mimicking cartilage arcade-like structure. *Biomolecules*. 2022 Dec 3; 12 (12): 1809. doi: 10.3390/biom12121809.
3. *Mirdamadi ES, Kalhori D, Zakeri N, Azarpira N, Solati-Hashjin M*. Liver tissue engineering as an emerging alternative for liver disease treatment. *Tissue Eng Part B Rev*. 2020 Apr; 26 (2): 145–163. doi: 10.1089/ten.teb.2019.0233.
4. *Zhang L, Guan Z, Ye JS, Yin YF, Stoltz JF, de Isla N*. Research progress in liver tissue engineering. *Biomed Mater Eng*. 2017; 28 (s1): S113–S119. doi: 10.3233/BME-171632.
5. *Wise JK, Yarin AL, Megaridis CM, Cho M.* Chondrogenic differentiation of human mesenchymal stem cells on oriented nanofibrous scaffolds: engineering the superficial zone of articular cartilage. *Tissue Eng Part A*. 2009 Apr; 15 (4): 913–921. doi: 10.1089/ten.tea.2008.0109.
6. *Daly AC, Kelly DJ.* Biofabrication of spatially organised tissues by directing the growth of cellular spheroids within 3D printed polymeric microchambers. *Biomaterials*. 2019 Mar; 197: 194–206. doi: 10.1016/j.biomaterials.2018.12.028.
7. *Schwab A, Hélary C, Richards RG, Alini M, Eglin D, D'Este M.* Tissue mimetic hyaluronan bioink containing collagen fibers with controlled orientation modulating cell migration and alignment. *Mater Today Bio*. 2020 Jun 1; 7: 100058. doi: 10.1016/j.mtbio.2020.100058.
8. *Lozinsky VI.* Polymeric cryogels as a new family of macroporous and supermacroporous materials for biotechnological purposes. *Russ Chem Bull*. 2008; 57 (5): 1015–1032. doi: 10.1007/s11172-008-0131-7.
9. *Lozinsky VI.* Cryostructuring of polymer systems. 50.† Cryogels and cryotropic gel-formation: terms and definitions. *Gels*. 2018; 4 (3): 77. doi: 10.3390/gels4030077.
10. *Henderson TMA, Ladewig K, Haylock DN, McLean KM, O'Connor AJ.* Cryogels for biomedical applications. *J Mater Chem B*. 2013; 1 (21): 2682–2695. doi: 10.1039/c3tb20280a.
11. *Memic A, Colombani T, Eggermont LJ, Rezaeeyazdi M, Steingold J, Rogers ZJ et al.* Latest advances in cryogel technology for biomedical applications. *Adv Ther*. 2019; 2 (4): 1800114. doi: 10.1002/adtp.201800114.
12. *Lozinsky VI.* Cryostructuring of polymeric systems. 55. Retrospective view on the more than 40-years studies performed in the A.N. Nesmeyanov Institute of Organoelement Compounds with respect of the cryostructuring processes in polymeric systems. *Gels.* 2020; 6 (3): 29. doi: 10.3390/gels6030029.
13. *Shiekh PA, Andrabi SV, Singh A, Majumder S, Kumar A.* Designing cryogels through cryostructuring of polymeric matrices for biomedical applications. *Eur Polym J.* 2021; 144; 110234. doi: 10.1016/j.eurpolymj.2020.110234.
14. *Ma Y, Wang X, Su T, Lu F, Chang Q, Gao J.* Recent advances in macroporous hydrogels for cell behavior and tissue engineering. *Gels*. 2022 Sep 21; 8 (10): 606. doi: 10.3390/gels8100606.
15. *Omidian H, Chowdhury SD, Babanejad N.* Cryogels: advancing biomaterials for transformative biomedical applications. *Pharmaceutics.* 2023 Jun 27; 15 (7): 1836. doi: 10.3390/pharmaceutics15071836.

16. *Lozinsky VI, Okay O*. Basic principles of cryotropic gelation. *Adv Polym Sci*. 2014; 263: 49–102. doi: 10.1007/978-3-319-05846-7_2.
17. *Sevastianov VI, Grigoriev AM, Basok YuB, Kirsanova LA, Vasilets VN, Malkova AP et al.* Biocompatible and matrix properties of polylactide scaffolds. *Russian Journal of Transplantology and Artificial Organs*. 2018; 20 (2): 82–90. (In Russ.). https://doi.org/10.15825/1995-1191-2018-2-82-90.
18. *Bhaskar B, Rao PS, Kasoju N, Nagarjuna V, Baadhe RR (Eds.)*. Biomaterials in Tissue Engineering and Regenerative Medicine. From Basic Concepts to State of the Art Approaches. Springer Nature Singapore Pte Ltd., 2021; 1039. https://doi.org/10.1007/978-981-16-0002-9.
19. *Sevastianov VI, Basok YB, Kirsanova LA, Grigoriev AM, Kirillova AD, Nemets EA et al.* A Comparison of the Capacity of Mesenchymal Stromal Cells for Cartilage Regeneration Depending on Collagen-Based Injectable Biomimetic Scaffold Type. *Life (Basel)*. 2021 Jul 27; 11 (8): 756. doi: 10.3390/life11080756.
20. *Sevast'yanov VI, Perova NV.* Biopolimernyy geterogennyy gidrogel' Sfero®GEL'' – in''ektsionnyy biodegradiruemyy implantat dlya zamestitel'noy i regenerativnoy meditsiny. *Prakticheskaya meditsina*. 2014; 8 (84): 120–126.
21. *DeQuach JA, Mezzano V, Miglani A, Lange S, Keller GM, Sheikh F, Christman KL.* Simple and high yielding method for preparing tissue specific extracellular matrix coatings for cell culture. *PLoS ONE.* 2010; 5 (9): e13039. doi: 10.1371/journal.pone.0013039.
22. *Lozinskiy VI, Kulakova VK, Kolosova OYu, Basok YuB, Grigor'ev AM, Perova NV, Sevast'yanov VI.* Biopolimernyy material dlya kletochno-inzhenernykh i/ili tkaneinzhenernykh konstruktsiy i sposob ego polucheniya. Pat. RF № 2774947 (2021); B.I. № 18 (2022).
23. *Grigoriev AM, Basok YuB, Kirillova AD, Surguchenko VA, Shmerko NP, Kulakova VK et al*. Cryogenically structured gelatin-based hydrogel as a resorbable macroporous matrix for biomedical technologies. *Russian Journal of Transplantology and Artificial Organs*. 2022; 24 (2): 83-93. https://doi.org/10.15825/1995-1191-2022-2-83-93.
24. *Lozinsky VI, Kulakova VK, Grigoriev AM, Podorozhko EA, Kirsanova LA, Kirillova AD et al*. Cryostructuring of polymeric systems: 63. Synthesis of two chemically tanned gelatin-based cryostructurates and evaluation of their potential as scaffolds for culturing of mammalian cells. *Gels.* 2022 Oct 28; 8 (11): 695. doi: 10.3390/gels8110695.
25. *Novikov I, Subbot A, Turenok A, Mayanskiy N, Chebotar I.* A rapid method of whole cell sample preparation for scanning electron microscopy using neodymium chloride. *Micron*. 2019; 124: 102687. doi: 10.1016/j.micron.2019.102687.
26. Mezhgosudarstvennyj standart GOST ISO 10993-5-2011 "Izdeliya medicinskie. Ocenka biologicheskogo dejstviya medicinskih izdelij. Chast' 5. Issledovanie na citotoksichnost': metody *in vitro*".

The article was submitted to the journal on 21.09.2023